Research on 3D map reconstruction of coal mine underground roadway based on lidar

Xuebin Qin, Wei Tang*, Yun Gao

College of Electrical and Control Engineering, Xi'an University of Science and Technology, Xi'an 710054, China

* Corresponding Author Email: 19064024900@163.com

Abstract. The underground coal mine environment is complex, the visual SLAM algorithm is not applicable in low light conditions, the underground roadway is narrow and long and the road surface is rugged. The traditional SLAM algorithm is prone to problems such as mismatching and cumulative errors, which affect the effect of mapping and positioning of inspection robots. Through the research of the A-LOAM algorithm of laser SLAM, combined with 16-line lidar, the 3D global map reconstruction of the underground crawler robot is studied. In the process of point cloud preprocessing, in order to solve the sparse point cloud of the A-LOAM algorithm in the coal mine scene, the Link 3D method is used to extract the point cloud features; in order to solve the cumulative error of SLAM mapping in the large-scale scene of the coal mine, Scan Context is used for loop detection, which improves the accuracy of the global map constructed and meets the requirements for mapping.

Keywords: Laser SLAM feature extraction, point cloud registration, loop detection.

1. Introduction

Simultaneous Localization and Mapping (SLAM) is a critical technology in autonomous driving for addressing mapping and localization challenges in harsh environments. Currently, 3D LiDAR-based SLAM algorithms are being widely applied to high-precision mapping tasks in coal mine environments [1]. The environmental map, which contains spatial information of the surroundings, serves as the fundamental basis for subsequent path planning and decision-making in autonomous systems, requiring real-time updates in response to dynamic changes. Simultaneously, pose information—comprising the position and orientation of autonomous equipment relative to the global map—must be continuously updated during operation to ensure accurate state estimation [2].

According to the existing industry guidance scheme and the research progress at home and abroad, this study takes the SLAM mapping algorithm of the underground roadway robot in coal mine as the starting point, and combines the complex environment of the underground roadway in the mining area to improve the accuracy of the robot map. The SLAM mapping algorithm of the traditional underground roadway inspection robot has the following challenges: 1. The underground lighting conditions are dark, and GPS cannot be directly applied in the coal mine, and the visual SLAM algorithm used on the ground is not strong in the weak light conditions underground. 2. LiDAR measurement has the problems of motion distortion, low-frequency update and point cloud sparsity, which determine that pure lidar is not conducive to robots to deal with aggressive movement or repetitive structures, such as coal mine roadways or narrow corridors. 3. The amount of data required in the mapping and positioning process is high, which makes the time complexity of the algorithm high and greatly reduces the operation efficiency.

After analyzing the aforementioned drawbacks, a laser algorithm suitable for underground applications has been proposed based on the original A-LOAM laser algorithm. This algorithm utilizes a 16-line laser radar for point cloud data acquisition. Building upon the original algorithm, the raw data from the laser radar is preprocessed, and the method of selecting key points using Link3D replaces the feature point extraction method in the original algorithm, providing strong constraints for the description of key points while reducing redundancy and ensuring computational efficiency.

In the backend optimization section, a Scan Context loop detection factor has been introduced to reduce the cumulative error during long-term mapping.

2. The improved A-LOAM algorithm is based on the 3D map reconstruction of the underground roadway environment in coal mines

This algorithm is based on the framework of the A-LOAM algorithm, and the overall framework of the improved algorithm is shown in Figure 1. This system uses LiDAR to receive raw point cloud data, performs downsampling on the raw point cloud data, and employs the A-LOAM algorithm's point cloud distortion correction method to eliminate the motion distortion of the LiDAR. Considering the sparsity and robustness of radar point clouds in underground coal mines, the Link 3D method is integrated during feature extraction, using robust neighboring key points to represent feature points, thereby accelerating the matching of feature points. In the backend optimization part, the Scan Context loop detection method is combined.

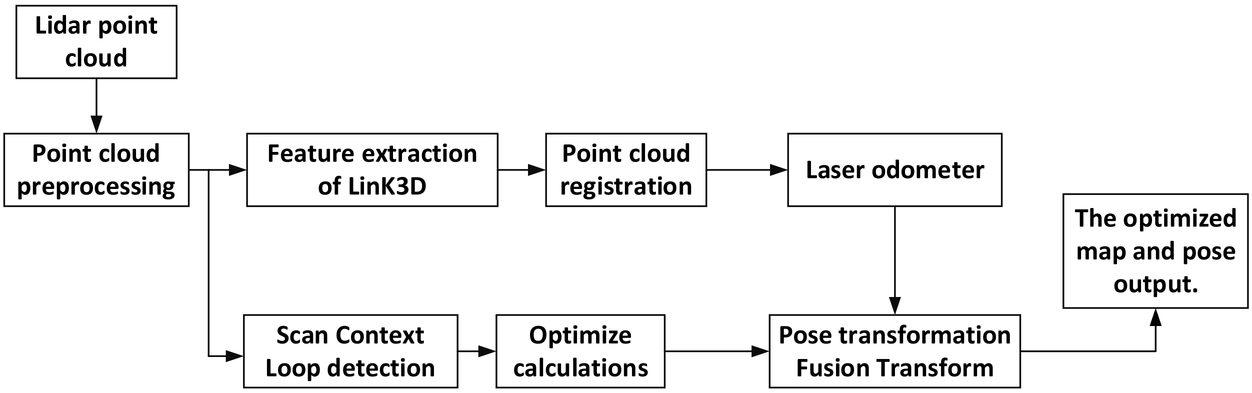

Fig. 1 Framework of algorithm

2.1 Data preprocessing

Due to the influence of environmental noise or equipment accuracy, there are outliers in the point clouds obtained by 3D lidar, which will cause inaccurate point cloud registration. The filtering of outliers is shown in the figure.

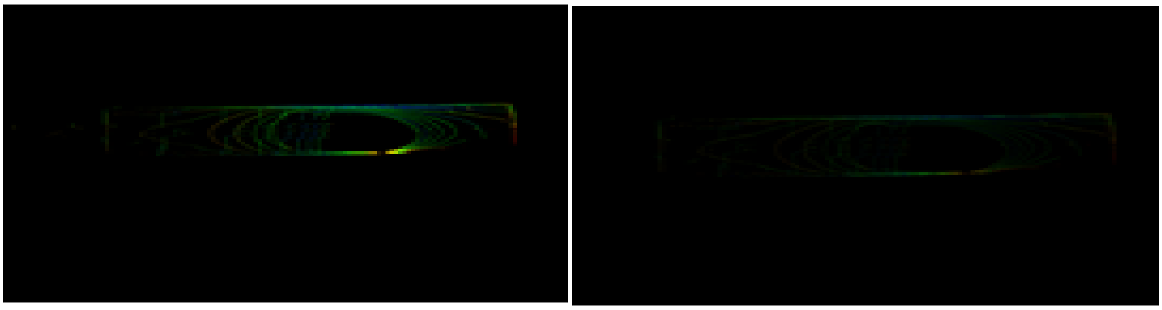

Fig. 2 Single frame point cloud after preprocessing

2.2 Point cloud feature extraction

During the feature point extraction process, the smoothness of the current point on the local surface varies. Given a three-dimensional LiDAR point cloud frame Pc, let i be any point in the current frame point cloud Pc. Ps is the set of continuous points along the same scan line as point i, uniformly distributed on both sides of point i, and |S| is the technical representation of the point cloud Ps. The smoothness of the current point i is defined as follows:

$$\nabla_i = \frac{1}{|S|} \| \sum_{j \in P_s, j \neq i} (\overrightarrow{p_j} - \overrightarrow{p_i}) \|^2 \tag{1}$$

where , $\overrightarrow{p_i}$ and $\overrightarrow{p_j}$ are the coordinates of two points i and j, respectively. The extracted edge points are greater than the threshold. The feature points extracted from the single-frame point cloud are shown in Figure 3.

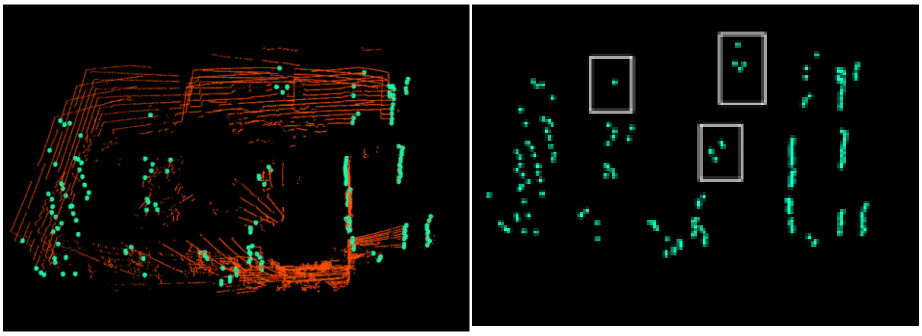

Fig. 3 Single frame radar point cloud feature point extraction

After obtaining the feature points, the ∇ of some points is greater than the set threshold, but they are not stable, as shown in the white box marks of the box in Figure 4. These points are scattered across the current point cloud scan frame, but may not be detected in the next scan, so the current points need to be filtered. Assuming that the z-axis is upward, the angle of the same feature point in the XoY plane of the LiDAR coordinate system is about the same, and the angle of pi is obtained:

$$\theta_{\mathrm{i}} = \arctan(\overrightarrow{p_i}.y / \overrightarrow{p_i}.x) \tag{2}$$

Guided by angular information, potential points are clustered in small groups rather than clustered across the area, and points with approximately the same horizontal angle are more likely to be on the same cluster. The angles of the XoY plane of the LiDAR coordinate system divide the points into 120 sectors, cluster them in the corresponding sectors, and use the centroid of each class as the key point of clustering for subsequent descriptor generation and point cloud inter-frame matching.

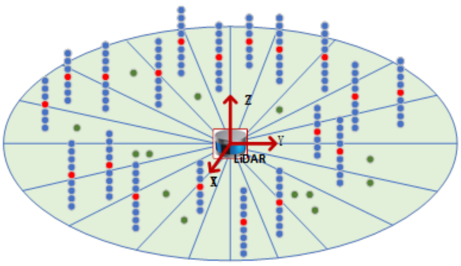

Fig. 4 Single frame point cloud feature point clustering

2.3 Point cloud registration

The level is divided into 180 sectors centered on the current key point k0, with one sector for each dimension of the descriptor. Inspired by the two-dimensional descriptor SIFT to search for the principal direction to ensure the pose invariant, the Link3D [3]principal direction is also searched and represented as the direction vector of the current key point k0 to k1, which is located in the first sector, and the rest of the sectors are sorted in counterclockwise order. Search for the nearest key to k0 in each sector. If the sector has a nearest key, the distance between the current key and the nearest key is used as the corresponding value for the descriptor, otherwise, the corresponding value of the descriptor for that sector is set to 0.

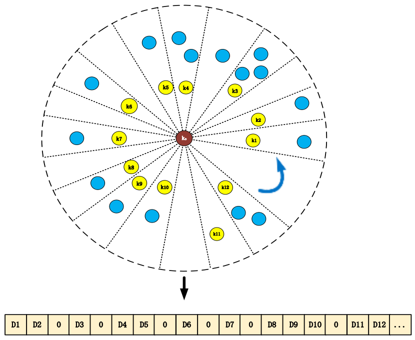

Fig. 5 Descriptor generation diagram

The direction from the current key k_0 to the other points $k_i(i \neq 1)$ is represented as $\overrightarrow{m_{0i}}$, using the angle between the Principal $\overrightarrow{m_{0i}}$ and the Principal to determine $\overrightarrow{m_{01}}$ which sector k_i it belongs to. The calculation method of the included angle is shown in equation (2):

$$\theta_i = \begin{cases} \arccos \dfrac{\overrightarrow{m_{01}} \bullet \overrightarrow{m_{0i}}}{|\overrightarrow{m_{01}}||\overrightarrow{m_{0i}}|} & if\ Di > 0 \\ 2\pi - \arccos \dfrac{\overrightarrow{m_{01}} \bullet \overrightarrow{m_{0i}}}{|\overrightarrow{m_{01}}||\overrightarrow{m_{0i}}|} & if\ Di < 0 \end{cases} \tag{3}$$

$$Di = \begin{vmatrix} x_1 & y_1 \\ x_i & y_i \end{vmatrix} \tag{4}$$

When generating a descriptor for a key, not only the nearest key is selected as the principal direction to generate the descriptor, but the second and third closest keys are selected as the principal direction to generate the descriptor, and then the priority is determined according to the distance between the principal key and the center key, and finally the value of the first non-0 value is extracted from the three descriptors according to the priority as the value of the final generated descriptor.

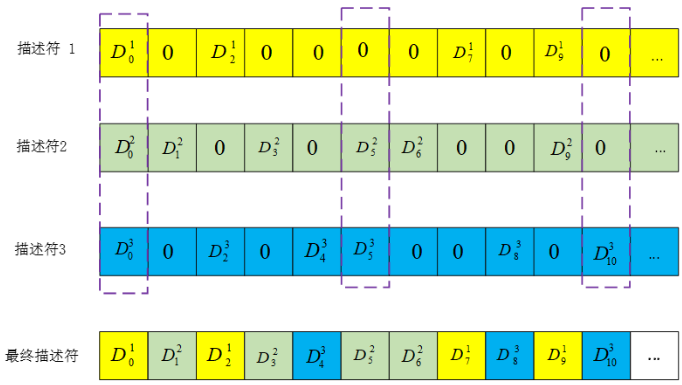

Fig. 6 Final descriptor generation for registration

In order to quickly measure the similarity of two descriptors, a calculation method similar to Hamming distance is used to define the similarity scores of the two LinK3D descriptors. They all calculate the corresponding dimensions. However, unlike Hamming's XOR operation, we only compute the non-zero dimensions of the two descriptors. Specifically, the absolute value of the difference between the corresponding non-zero dimensions is calculated in two descriptors. If the value is less than 0.2, the similarity score increases by 1. A match is considered valid if its similarity score is above the threshold.

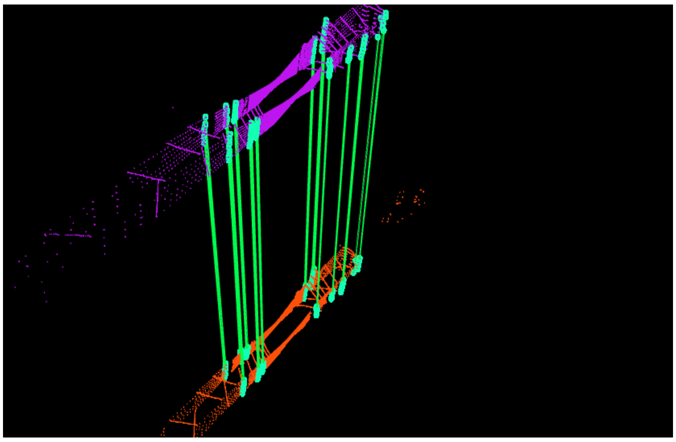

Fig. 7 Point cloud interframe registration map

2.4 Loop detection

Loopback detection is an important part of the SLAM system to correct the mapping error, which optimizes the cumulative error generated by the lidar by detecting the robot passing through a known area. Scan Context [4] is a Lidar-based environment recognition and localization method, which does not rely on histograms and pre-training, directly records the 3D structure from the LiDAR scan space, uses the similarity score to calculate the distance between the two scanning contexts, and uses a two-stage search algorithm to detect the formed loop.

The steps for integrating Scan Context are as follows: For the processed single-frame radar point cloud, extract the Scan Context descriptor, project the generated descriptor into polar coordinates, and use the Ring Key to extract the mean of the row vectors and the Secor Key to extract the mean of the column vectors. The KD Tree search algorithm is employed to find candidate Scan Contexts, and by calculating the most similar Scan Context, the pose of the LiDAR is adjusted to correct the mapping error of the two frames of data in the same polar coordinate system.

3. Experiment

3.1 Quantitative analysis of the M2DGR dataset

The M2DGR[5] dataset is a dataset provided by Shanghai Jiao Tong University for the accuracy evaluation of SLAM for ground robots. The dataset includes panoramic RGB cameras, infrared cameras, event cameras, Velodyne-32 line lidars, IMU inertial measurement units, and GNSS global navigation satellite data.

The performance of the proposed algorithm is verified by the hall_02 sequence in indoor scenes, and the ground truth trajectory information of the sequence is collected by the mobile robot moving freely indoors, and the algorithm and A-LOAM are evaluated in the sequence.

Table 1. Absolute trajectory error of the previous algorithm was improved

	Index	Value/m
APE before improvement	max	0.6426
	min	0.0258
	mean	0.2709
	rmse	0.2971
	std	0.1220

Table 2. Absolute trajectory error of the improved algorithm

	Index	Value/m
APE before improvement	max	**0.4824**
	min	0.0343
	mean	**0.2487**
	rmse	**0.2678**
	std	**0.0993**

As can be seen from Table 1 and Table 2, the maximum value of max, mean mean, root mean square error and standard deviation of the improved algorithm are reduced compared with the previous algorithm, which indicates that the improved algorithm has higher accuracy and robustness, and provides a reliable map for subsequent robot relocation.

3.2 Qualitative analysis of self-collected datasets

The equipment used in this algorithm is as follows:

The operating system is Ubuntu 18.04 and the ROS environment is melodic.

Computer Hardware: Intel(R) Core(TM) i9-12000H CPU, 8GB RAM, 1T SS.

Compiled language: C++. Sensor: RobSense-16, WHEELTC-N100 nine-axis IMU.

The data acquisition environment is the underground simulated roadway in the coal mining area.

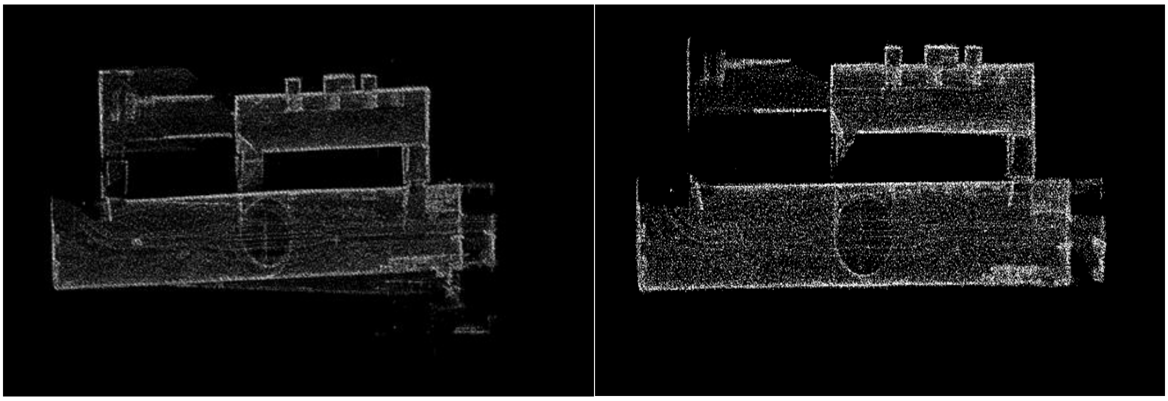

Fig. 8 PCD map of underground roadway and hydropower room

The qualitative analysis of the effects before and after the improvement of the text is shown in Figure 8. The aforementioned experiments are the test results of the 16-line laser radar from Sutech Juchuang in the underground tunnels of the coal mine, and it can be observed that the algorithm before the improvement exhibits the phenomenon of map ghosting. After the improvement, the ghosting phenomenon disappears, allowing for a complete representation of the underground tunnels of the coal mine.

4. Summary

This study proposes an improved map reconstruction algorithm for mine tunnel inspection robots, building upon the classical laser SLAM framework of the A-LOAM algorithm. The proposed system employs a RoboSense 16 multi-line LiDAR for raw point cloud acquisition. After implementing noise reduction and filtering preprocessing on the raw data, the Link 3D method is utilized for feature extraction in coal mine tunnels. This approach establishes robust constraints for keypoint descriptors while effectively reducing computational redundancy. For backend optimization, Scan Context loop closure detection is integrated to mitigate cumulative errors, thereby establishing a reliable foundation for subsequent robotic path planning in underground coal mine environments.

References

[1] Zhang Qing Yu, Cui Lin Zhen, Du Xiu Duo, et al. 3D LiDAR SLAM algorithm for mapping and localization in mining environments[J]. Bulletin of Surveying and Mapping, 2023(5): 72-77.

[2] Cui Shao Yun,Bao Jiu Sheng,Hu De Ping,et al. The research status and development trend of SLAM technology and its application in the field of unmanned mine driving [J]. Industrial and mining automation,2024,50(10):38-52.

[3] Cui, Yunge, et al. "Link3d: Linear keypoints representation for 3d lidar point cloud." IEEE Robotics and Automation Letters (2024).

[4] Kim G , Kim A .Scan Context: Egocentric Spatial Descriptor for Place Recognition Within 3D Point Cloud Map[C]//2018 IEEE/RSJ International Conference on Intelligent Robots and Systems (IROS).IEEE, 2018.

[5] [1] Yin J , Li A , Li T ,et al.M2DGR: A Multi-Sensor and Multi-Scenario SLAM Dataset for Ground Robots[J].IEEE Robotics and Automation Letters, 2022, 7(2).